Altered intra- and inter-network brain functional connectivity in upper-limb amputees revealed through independent component analysis

https://doi.org/10.4103/1673-5374.339496

Date of submission: October 13, 2021

Date of decision: January 7, 2022

Date of acceptance: February 18, 2022

Date of web publication: April 29, 2022

Bing-Bo Bao[1, #], Hong-Yi Zhu[1, #], Hai-Feng Wei[1], Jing Li[2], Zhi-Bin Wang[2], Yue-Hua Li[2], Xu-Yun Hua[3], Mou-Xiong Zheng[3], Xian-You Zheng[1, *]

From the Contents

Graphical Abstract *ICA of brain connectivity after amputation*

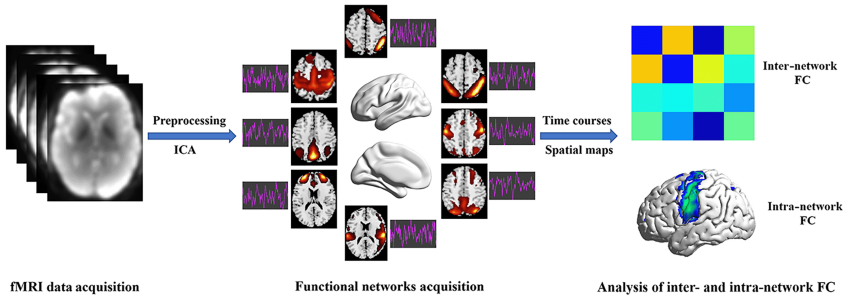

Abstract

Although cerebral neuroplasticity following amputation has been observed, little is understood about how network-level functional reorganization occurs in the brain following upper-limb amputation. The objective of this study was to analyze alterations in brain network functional connectivity (FC) in upper-limb amputees (ULAs). This observational study included 40 ULAs and 40 healthy control subjects; all participants underwent resting-state functional magnetic resonance imaging. Changes in intra- and inter-network FC in ULAs were quantified using independent component analysis and brain network FC analysis. We also analyzed the correlation between FC and clinical manifestations, such as pain. We identified 11 independent components using independent component analysis from all subjects. In ULAs, intra-network FC was decreased in the left precuneus (precuneus gyrus) within the dorsal attention network and left precentral (precentral gyrus) within the auditory network; but increased in the left Parietal_Inf (inferior parietal, but supramarginal and angular gyri) within the ventral sensorimotor network, right Cerebelum_Crus2 (crus II of cerebellum) and left Temporal_Mid (middle temporal gyrus) within the ventral attention network, and left Rolandic_Oper (rolandic operculum) within the auditory network. ULAs also showed decreased inter-network FCs between the dorsal sensorimotor network and ventral sensorimotor network, the dorsal sensorimotor network and right frontoparietal network, and the dorsal sensorimotor network and dorsal attention network. Correlation analyses revealed negative correlations between inter-network FC changes and residual limb pain and phantom limb pain scores, but positive correlations between inter-network FC changes and daily activity hours of stump limb. These results show that post-amputation plasticity in ULAs is not restricted to local remapping; rather, it also occurs at a network level across several cortical regions. This observation provides additional insights into the plasticity of brain networks after upper-limb amputation, and could contribute to identification of the mechanisms underlying post-amputation pain.

Key Words: amputation; functional connectivity; functional magnetic resonance imaging; independent component analysis; neuroimaging; phantom pain; phantom sensation; resting-state networks

Introduction

The human brain continuously adapts to physical and environmental changes, ranging from small local functional changes to large structural changes (Edde et al., 2021). It is also now clear that the occurrence and development of many diseases are accompanied by changes in brain function and brain structure. Therefore, understanding the processes underlying disease-related changes in brain function is not only useful for understanding a disease, but also for identifying new diagnostic criteria, prevention strategies, and treatment methods for diseases that manifest in the brain (Heneka et al., 2018; Barth and Ray, 2019; Hortobágyi et al., 2021).

Amputation is a treatment option for severe limb trauma, limb tumor, or limb vascular disease (Qureshi et al., 2020). Although amputations can help patients survive, amputees still face many complications, including phantom limb sensation, phantom limb pain (PLP), and residual limb pain (RLP) (Stankevicius et al., 2021). In addition, many amputees experience varying degrees of mood disorders, including anxiety and depression, which can also interfere with their ability to return to work and engage in social activities (McKechnie and John, 2014). From a lay point of view, it may seem that amputation "cures" the patient's disease. However, amputation and the resulting limb denervation inevitably lead to local or global changes in brain function, which may manifest as pain and/or changes in emotion and cognition, for example (Makin and Flor, 2020). Therefore, amputees are faced not only with the loss of the limb itself, but also with changes in brain function caused by the loss of that limb.

Various imaging techniques, such as functional magnetic resonance imaging (fMRI), electroencephalography, magnetoencephalography, and positron emission computed tomography, have been used to assess brain function abnormalities after amputation (Collins et al., 2018). One widely used, noninvasive method for assessing the function of regional and local neural

[1]Department of Orthopedic Surgery, Shanghai Jiao Tong University Affiliated Sixth People's Hospital, Shanghai, China; [2]Institute of Diagnostic and Interventional Radiology, Shanghai Jiao Tong University Affiliated Sixth People's Hospital, Shanghai, China; [3]Department of Traumatology and Orthopedics, Yueyang Hospital, Shanghai University of Traditional Chinese Medicine, Shanghai, China

*Correspondence to: Xian-You Zheng, MD, PhD, zhengxianyou@126.com.

https://orcid.org/0000-0002-9770-5394 (Xian-You Zheng)

#These two authors contributed equally to this paper.

Funding: *This study was supported by the National Natural Science Foundation of China, No. 81974331 (to XYZ), Shanghai Municipal Education Commission-Gaofeng Clinical Medicine Grant, No. 20161429 (to XYZ).*

How to cite this article: *Bao BB, Zhu HY, Wei HF, Li J, Wang ZB, Li YH, Hua XY, Zheng MX, Zheng XY (2022) Altered intra- and inter-network brain functional connectivity in upper-limb amputees revealed through independent component analysis. Neural Regen Res 17(12):2725-2729.*

circuitry in the brain is resting-state fMRI (rs-fMRI) (Yang et al., 2020). Given that the mechanisms underlying pain in amputees remain somewhat obscure, in recent years, many studies have focused on establishing central nervous system theories to explain PLP (Wall et al., 2002; Makin et al., 2015). The most popular central nervous system theory is the cortical remapping theory, which explains post-amputation pain from the perspective of brain functional plasticity (Flor et al., 1995; Collins et al., 2018). Most previous studies, however, have limited their efforts to brain regions that are local to the somatotopic region of the amputated limb (Bao et al., 2021), especially sensorimotor regions and sensorimotor networks, and have failed to consider possible changes in whole-brain intra- and inter-network connectivity (Boccia et al., 2020). Moreover, the small number of amputation subjects in previous studies has limited the results.

Independent component analysis (ICA) is a data-driven method for delineating brain-wide, spatially independent patterns of coherent signals (Wang et al., 2014; Smitha et al., 2017). In its essence, ICA is a computational method for separating a multivariate signal into its unique components that are statistically and spatially independent from each other. For the case of human brain activity, ICA separates fMRI data into spatially independent patterns of activity (McKeown and Sejnowski, 1998). The unique advantage of ICA over seed-based functional connectivity (FC) analysis is that ICA enables researchers to directly measure interactions within and between multiple brain networks. In recent years, ICA intra-network and inter-network analyses have been used effectively to study the pathogenesis of many diseases, such as stroke (Zhao et al., 2018), Parkinson's disease (Peraza et al., 2017; Caspers et al., 2021), and Alzheimer's disease (Zhan et al., 2016). However, ICA studies examining FC changes within and between resting-state networks (RSNs) in upper-limb amputees (ULAs) are rare.

In the present study, we quantified large-scale functional reorganization in the brains of ULAs by using ICA-based RSN analysis methods and by investigating intra-network and inter-network connectivity. We hypothesized that intra-network and inter-network FC is appreciably altered in ULAs compared with that in healthy controls (HCs). Our aim was to determine whether changes in intra-network and inter-network resting-state connectivity underlie neurobehavioral symptoms experienced by ULAs, in particular PLP. We also investigated correlations between clinical behavioral measures and altered resting-state FC. To our knowledge, this rs-fMRI study in ULAs is the first of its kind to use an ICA-based approach to elucidate the mechanisms underlying PLP.

Participants and Methods

Participants

Participants in the ULA group comprised 40 individuals (32 male and 8 female; mean age ± SD: 45.23 ± 9.05 years) that had undergone unilateral upper-limb amputation (22 patients with dominant right-side amputations) at the Shanghai Jiao Tong University Affiliated Sixth People's Hospital between October 2020 and May 2021. Of the 40 amputations, 23 were below the elbow, and 17 were above the elbow. All potential participants were screened according to the following inclusion criteria: (1) aged 18–60 years (this age setting was determined by our trial design, which took into account the potential limitations of brain remodeling in older subjects); and (2) unilateral upper-limb amputation after traumatic injury. The exclusion criteria were as follows: (1) upper-limb amputation accompanied by other limb injuries; (2) history of neurological disease; (3) pre-existing psychiatric or neurological disorders; (4) history of using psychotropic drugs; (5) left-handed; and (6) contraindications identified on MRI.

Forty healthy individuals who met the same age requirements and exclusion criteria as the amputation group, and were matched for age (mean age ± SD: 47.23 ± 8.84 years), education, and sex, served as the HCs. All healthy controls were from the community and were given free MRI scans in our hospital between October 2020 and May 2021. Handedness was assessed using a language-appropriate version of the Edinburgh Handedness Inventory (Yang et al., 2018); the dominant hand of all participants (40 ULAs and 40 HCs) was the right hand.

Detailed medical information was collected for all amputees, including amputation level; amputation side; length of time (months) between amputation and enrollment in our study; daily activity hours of the stump limb, including active activity (deliberate functional rehabilitation and coping with everyday life) and passive activity (such as wearing prosthesis); other treatment approaches received before enrollment; and efficacy of those treatments. We also used a visual analog scale based on one described by (Makin et al., 2013) to assess and quantify RLP and PLP (0, "no pain"; 10, "worst pain imaginable").

Ethical approval and informed consent

This prospective observational study was approved by the Ethics Committee of Shanghai Jiao Tong University Affiliated Sixth People's Hospital of China (approval No. 2017-034), registered with the Chinese Clinical Trial Registry (registration no. ChiCTR1900025882), and performed in accordance with the ethical standards laid down in the 1964 *Declaration of Helsinki* and its later amendments. All participants gave informed consent prior to inclusion in this study.

MRI scanning and image acquisition

All images were acquired using a Siemens 3.0-Tesla MRI scanner (MAGNETOM Prisma; Siemens Healthcare GmbH, Erlangen, Germany) equipped with a 64-channel phased-array head coil by a senior radiologist in our hospital. During image acquisition, subjects were instructed to relax but remain awake, to close their eyes during the entire scanning period, and to try not to think of anything. To reduce head movement artifacts, the subject's head was placed in a padded foam collar, and the subject wore earplugs to minimize loud startling noise from the scanner during image acquisition. A three-dimensional magnetization-prepared, rapid gradient echo sequence was used to record structural images using the following acquisition parameters: repetition time = 2300 ms; echo time = 2.46 ms; flip angle = 8°; matrix = 256 × 256 mm^2; slice thickness = 1.0 mm; voxel size = 1.0 × 1.0 × 1.0 mm^3. A total of 176 slices were acquired for each subject session. An echo-planar imaging sequence was used to record functional images with the following acquisition parameters: repetition time = 1200 ms; echo time = 39 ms; flip angle = 52°; matrix = 88 × 88; field of view = 210 mm; slice thickness = 2.4 mm; 56 slices, voxel size = 2.4 mm × 2.4 mm × 3.0 mm. After a scanning time of 288 seconds, we collected 240 volumes. None of the subjects mentioned experiencing any significant discomfort during or after scanning. The radiologist was well aware of the trial, but not of the patient's details, such as the timing of the amputation or the degree of pain.

Data preprocessing

Preprocessing was performed using Statistical Parametric Mapping software (SPM12; http://www.fil.ion.ucl.ac.uk/spm) implemented in MATLAB R2013b (MathWorks Inc., Natick, MA, USA). Data preprocessing comprised six steps. First, we discarded the first 10 volumes of each subject's data set; this number was sufficient to allow the scanner to reach magnetization equilibrium and for the subject to adapt to the scanner environment. Second, we manually set the anterior commissure as a reference point, and then aligned the remaining 230 images of each subject with their anatomical data sets. Third, to correct for head motion during scanning, we calculated the subject's head motion parameters by estimating the translation in the *x*, *y*, and *z* directions and the angular rotation at each axis for each volume. We excluded from data of subjects whose heads moved > 2.0 mm in any direction and rotated > 2.0° (Power et al., 2014). Fourth, in the normalization step, we co-registered each subject's structural images with their mean functional image, which was divided into gray matter, white matter, and cerebrospinal fluid. Fifth, we spatially normalized the functional images according to the Montreal Neurological Institute (MNI) space/coordinate system using the deformation parameters estimated above, and then resampled them into a 3-mm cubic voxel. Finally, to decrease spatial noise, we spatially normalized and smoothed all data sets using the full width at half maximum of 6 mm of the Gaussian kernel.

Independent component analysis

Participants' data were assessed by ICA using GIFT software (Version 4.0b, http://mialab.mrn.org/software/gift/). GIFT software automatically estimates the number of independent components (N = 23) using the minimum description length criteria. The data are then broken down by spatial ICA into linear mixtures of components that are spatially independent and that display unique time course profiles. In the present study, we accomplished this decomposition by reducing the data in two steps. First, subject-specific data were reduced into 39 principal components using principal component analysis. Second, these components were linked (concatenated) across time and then reduced (decomposed) further into 23 independent components using the infomax algorithm. We repeated the infomax algorithm 100 times in ICASSO (http://research.ics.tkk.fi/ica/icasso/) to ensure estimate stability, and then selected the most central run for further analysis. Finally, we used the group ICA back-reconstruction approach to compile spatial maps and time courses for each participant. From these analyses, we were able to identify several independent components (i.e., functional networks) exhibiting peak activations in gray matter; low spatial overlap with known artifacts (e.g., vascular, motion, susceptibility); and mainly low-frequency power. This method identified 11 functional networks from the 23 independent components derived from the second decomposition step.

Data analysis

Analysis of demographic and clinical characteristics

After determining that our data were normally distributed, we evaluated demographic and clinical data of ULAs and HCs using two-tailed two sample *t*-tests and chi-square test (only the sex variable was tested) (SPSS 24.0; IBM, Armonk, NY, USA). $P < 0.05$ was designated as significant.

Analysis of intra-network functional connectivity

We created a component map and a network mask for each participant by performing a one-sample *t*-test on the independent component of each ULA and HC using GIFT software (Version 4.0b, http://mialab.mrn.org/software/gift/). The false discovery rate (FDR) method ($P < 0.05$) was used to correct for multiple comparisons. For each component, we obtained a total MASK by further combining the masks of each ULA and HC. A two-sample *t*-test with regressing covariates (age, education, and sex) was conducted. To compare FC differences in each component of ULAs versus HCs within the corresponding network mask, we performed a two-sample *t*-test using regressing covariates (age, education, and sex). The AlphaSim correction ($P < 0.001$) was used to correct the multiple comparison results (Ledberg et al., 1998).

Analysis of inter-network functional connectivity

We examined fluctuations in the pattern of inter-network FCs by computing the temporal correlation across different RSNs. First, we obtained the time course of each RSN from the ICA procedure. Next, we used the time courses

of each pair of the 11 RSNs to compute the temporal correlation, namely functional network connectivity. The resulting functional network connectivity results were then normalized using the Fisher r-to-z transformation to meet a normal distribution, and obtain an 11 × 11 matrix inter-network FC within RSNs. Finally, to evaluate functional network connectivity differences between ULAs and HCs, we subjected the matrix to a two-sample *t*-test; FDR ($P < 0.05$) was used to correct the multiple comparison results.

Correlation analysis

Correlation analyses were conducted to determine and quantify the relationship between intra-network FC, inter-network FC, and clinical variables. We used the following data in our analyses: intra-network FC, inter-network FC, RLP scores, PLP scores, amputation level, and ULAs' daily activity hours of the stump limb. After controlling for certain variables (e.g., age, sex, educational level, and amputation time), we performed a two-tailed partial correlation analysis; $P < 0.05$ was considered statistically significant.

Results

Clinical and demographic characteristics of participants

Clinical and demographic clinical characteristics of participants (ULAs and HCs) are shown in **Table 1**. Statistical analysis of participants' clinical and demographic data failed to identify any significant between-group differences in age, sex, or education ($P > 0.05$).

Resting-state network components

We identified various RSN components in line with previously described methods (Smith et al., 2009). The following 11 independent components were identified: anterior default mode network, posterior default mode network, dorsal attention network (DAN); ventral attention network (VAN); dorsal sensorimotor network (dSMN); ventral sensorimotor network (vSMN); left frontoparietal network, right frontoparietal network (rFPN); and medial visual network, posterior visual network, auditory network (**Figure 1**).

Altered FC within resting-state networks

In ULAs, multiple RSNs displayed significant FC differences compared with those in HCs ($P < 0.001$, AlphaSim-corrected; **Figure 2** and **Table 2**). In the DAN, the left precuneus (precuneus gyrus) showed decreased FC. In the vSMN, the left Parietal_Inf (inferior parietal, but supramarginal and angular gyri) showed increased FC. In the ventral attention network, the right Cerebelum_Crus2 (crus II of cerebellum) and left Temporal_Mid (middle temporal gyrus) showed increased FC. In auditory network, the left precentral (precentral gyrus) showed decreased FC, but the left Rolandic_Oper (rolandic operculum) showed increased FC.

Altered inter-network functional connectivity

In ULAs, the three following pairs of networks showed decreased inter-network FC compared with that in HCs: dSMN and vSMN, dSMN and rFPN, and dSMN and DAN ($P < 0.05$, FDR-corrected; **Figure 3**).

Correlation analysis results

In the ULA group, dSMN-vSMN FC and RLP scores were negatively correlated ($r = -0.655$, $P < 0.001$; **Figure 4A**), and dSMN-vSMN FC and PLP scores were negatively correlated ($r = -0.695$, $P < 0.001$; **Figure 4B**). In addition, in the ULA group, dSMN-vSMN FC and daily activity hours of the stump limb were positively correlated ($r = 0.718$, $P < 0.001$; **Figure 4C**).

Table 1 | **Demographic and clinical characteristics of participants**

Characteristics	ULA ($n = 40$)	HC ($n = 40$)	t/χ^2	*P*
Age (years)	45.23±9.05	47.23±8.84	1	0.768
Education (years)	7.85±4.73	7.98±4.53	0.121	0.703
Sex (female/male)	8/32	11/29	0.623	0.6
Hand dominance (left/right)	0/40	0/40	–	
Amputation side (left/right)	18/22	–	–	
Amputation location: above/below elbow	17/23	–	–	
Time since amputation (months)	73.85±24.46 (6–124)	–	–	
Age at amputation (years)	39.35±9.52 (21–59)	–	–	
RLP scores	4.58±2.46 (0–9)	–	–	
PLP scores	5.23±2.76 (0–10)	–	–	
Stump limb daily activity hours	4.40±3.05 (0–13)	–	–	

Values are expressed as the mean ± SD, mean ± SD (range) or number/number. HC: Healthy control; PLP: phantom limb pain; RLP: residual limb pain; ULA: upper limb amputee.

Table 2 | **Brain regions with significant differences in intra-network FC between ULAs and HCs**

				MNI coordinates		
Regions	Side	Peak T value	Cluster size	*X*	*Y*	*Z*
DAN						
Precuneus	L	–3.951	19	–12	–66	51
vSMN						
Parietal_Inf	L	4.421	16	–51	–39	45
VAN						
Cerebelum_Crus2	R	4.376	17	42	-69	–45
Temporal_Mid	L	4.296	19	–60	–15	0
AN						
Rolandic_Oper	L	4.309	20	–57	3	6
Precentral	L	–4.543	24	–36	–9	54

$n = 40$ in ULA and HC, respectively. AN: Auditory network; Crus2: crus II of cerebellum; DAN: dorsal attention network; L: left; MNI: Montreal Neurological Institute; Parietal_Inf: inferior parietal, but supramarginal and angular gyri; Precentral: precentral gyrus; Precuneus: precuneus gyrus; R: right; Rolandic_Oper: rolandic operaculum; Temporal_Mid: middle temporal gyrus; VAN: ventral attention network; vSMN: ventral sensorimotor network.

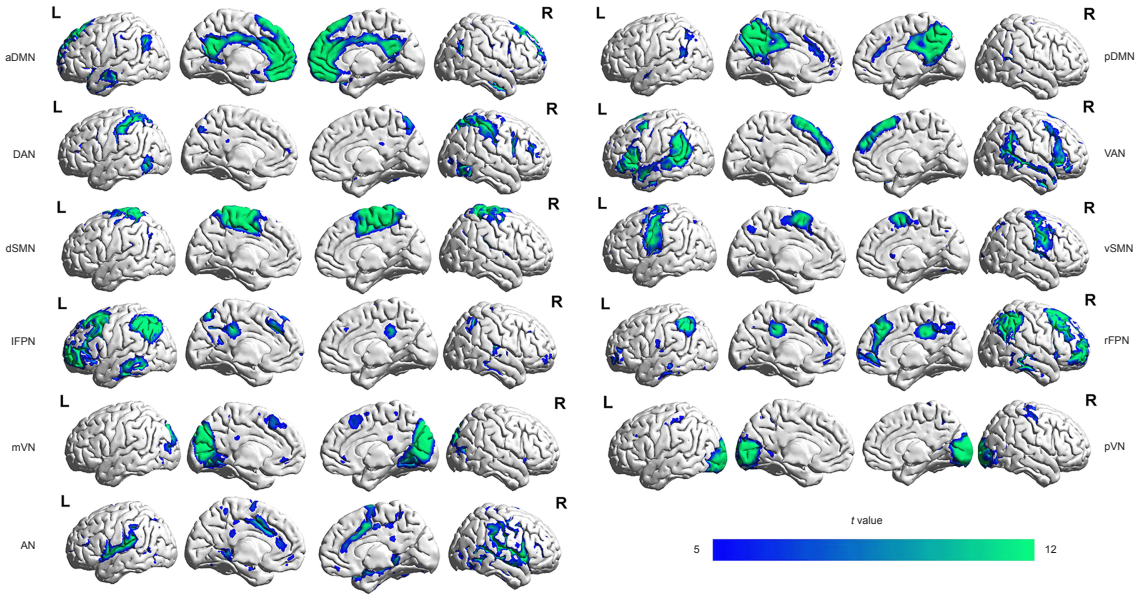

Figure 1 | **Spatial maps of 11 selected functional networks in upper-limb amputees and healthy controls using independent component analysis.**
The colored bars indicate the *t*-values of the one-sample *t*-test of all subjects ($P < 0.05$, false discovery rate-corrected). aDMN: Anterior default mode network; AN: auditory network; DAN: dorsal attention network; dSMN: dorsal sensorimotor network; lFPN: left frontoparietal network; L: left; mVN: medial visual network; pDMN: posterior default mode network; pVN: posterior visual network; R: right; rFPN: right frontoparietal network; VAN: ventral attention network; vSMN: ventral sensorimotor network.

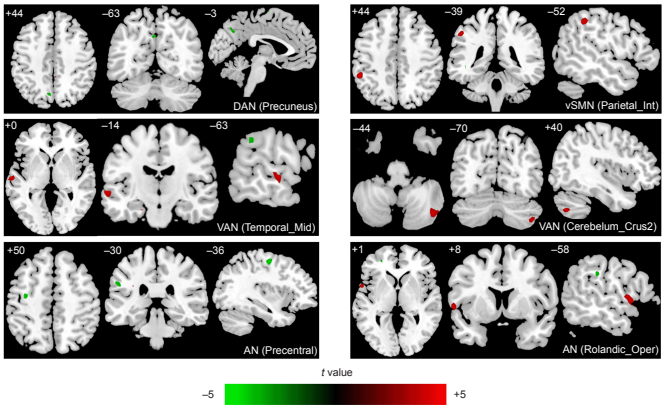

Figure 2 | Brain regions with significant differences in intra-network FC between upper-limb amputees and healthy controls by two-sample *t*-tests.
Warm and cold colors indicate regions with higher or lower intra-network FC in upper-limb amputees compared with healthy controls ($P < 0.001$, AlphaSim-corrected). The colored bars indicate the *t*-values of the two-sample *t*-tests. AN: Auditory network; DAN: dorsal attention network; FC: functional connectivity; VAN: ventral attention network; vSMN: ventral sensorimotor network.

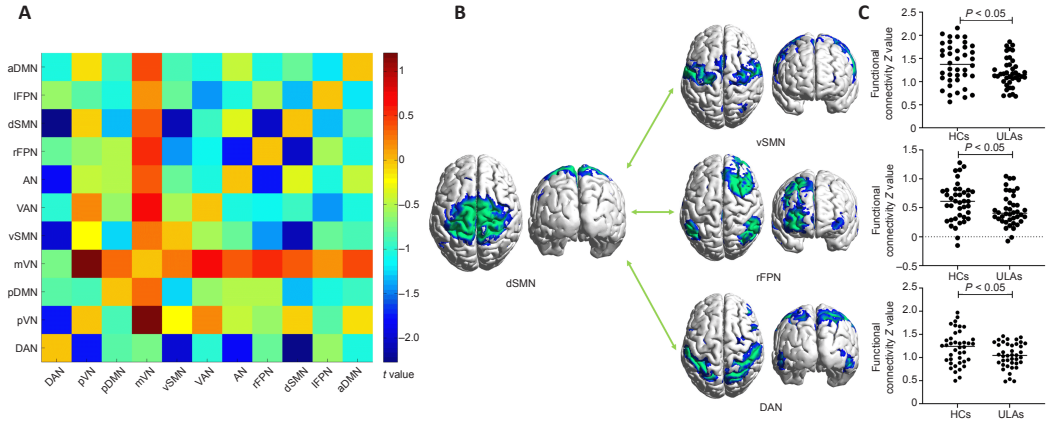

Figure 3 | Altered inter-network FC in upper-limb amputees.
(A) Heat map showing inter-network FC between pairs of regions in upper-limb amputees. Warm and cold colors indicate regions with higher or lower inter-network FC. (B) Three-dimensional renderings of the brain showing the statistical significance networks of inter-network FC. FC was decreased between the dSMN and the vSMN, rFPN, and DAN ($P < 0.05$, FDR-corrected). (C) Dot plots showing inter-network FC in healthy controls (HCs) and upper-limb amputees (ULAs) using two-sample *t*-tests. aDMN: Anterior default mode network; AN: auditory network; DAN: dorsal attention network; dSMN: dorsal sensorimotor network; FC: functional connectivity; FDR: false discovery rate; lFPN: left frontoparietal network; mVN: medial visual network; pDMN: posterior default mode network; pVN: posterior visual network; rFPN: right frontoparietal network; VAN: ventral attention network; vSMN: ventral sensorimotor network.

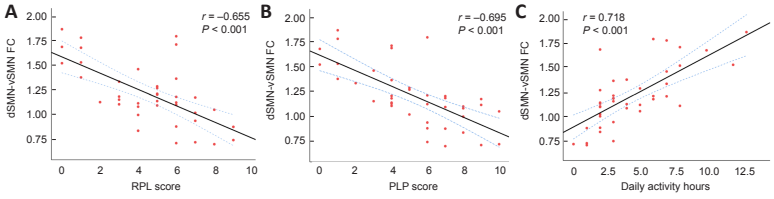

Figure 4 | Significant correlations between inter-network FC and clinical assessments in ULAs (two-tailed partial correlation analysis).
(A) Scatter plot showing a statistically significant linear relationship between dSMN-vSMN FC and RLP scores in the ULA group ($r = –0.655$, $P < 0.001$). (B) Scatter plot showing statistically significant linear relationship between the dSMN-vSMN FC and PLP scores in the ULA group ($r = –0.695$, $P < 0.001$). (C) Scatter plot showing statistically significant linear relationship between dSMN-vSMN FC and daily activity hours of stump limb in the ULA group ($r = 0.718$, $P < 0.001$). dSMN: Dorsal sensorimotor network; FC: functional connectivity; PLP: phantom limb pain; RLP: residual limb pain; ULA: upper-limb amputee; vSMN: ventral sensorimotor network.

Discussion

To our knowledge, this is the first exploratory study to analyze intra- and inter-network FC and their correlations in ULAs. Depending on the ICA approach, in ULAs, we found that 4 of the 11 well-known RSNs were abnormal, including attention, sensorimotor, and auditory networks. At the brain-network level in ULAs, we observed decreased inter-network FC in sensorimotor and high attention networks. Correlation analysis revealed that this decrease in brain-network FC was correlated with certain clinical manifestations, such as the ULAs' RLP scores, PLP scores, and daily activity hours of the stump limb. Together, these findings support our hypothesis that intra-network and inter-network FC in ULAs is altered compared with that in HCs. The present findings also enhance and clarify our current understanding of the processes involved in pathophysiological changes that occur following amputation. Most importantly, we found that amputation induces reorganization in sensorimotor networks, which disrupts related networks that underlie sensorimotor behavior. This supports the notion that there is a common mechanism underlying network FC alternations following amputations.

A large percentage of limb amputees suffer from PLP and phantom limb sensation after amputation (Sherman et al., 1984), which considerably impairs their quality of life. Of 2750 respondents in a survey of military veteran amputees, 78% reported PLP (Limakatso et al., 2020). In a systematic review of all-cause amputations, a PLP prevalence rate of 64% was estimated (Limakatso et al., 2020). Despite this, the pathogenesis of PLP and phantom limb sensation remain unclear. To address this issue, more recent research has focused on brain functional remodeling in amputees, with the aim of identifying the underlying changes in FC that might lead to treatments for their pain and paresthesia. At present, we have a relatively complete picture of the central mechanism responsible for PLP (Flor et al., 1995; Kuffler, 2018; Makin and Flor, 2020). This understanding has led to the development of amputation rehabilitation techniques, such as transcranial magnetic stimulation (Nardone et al., 2019), mirror therapy (Chan et al., 2019), and direct current stimulation (Kikkert et al., 2019). Among the numerous studies on brain functional remodeling, sensorimotor remodeling is favored by many researchers as a starting point for therapy. Although the sensorimotor area that represents the amputated limb is not lost after amputation, the loss of physical stimulation to that limb initiates a series of functional and structural changes in that particular sensorimotor area (Melzack, 2001; Pacheco-Barrios et al., 2020).

Our findings revealed a significant decline in FC both within and between sensorimotor brain networks, which provides further support for the presence of a central remodeling mechanism after amputation. Our correlational analyses also revealed that the decreased FC between the dSMN and vSMN was significantly and negatively correlated with RLP and PLP. This indicates that the maintenance of FC between sensorimotor networks may improve post-amputation pain to some extent, but further research on this is needed given that this was only a correlation. Interestingly, we also found a significant positive correlation between daily stump activity hours and FC within sensorimotor networks in amputees. Recent studies have shown that engaging in sports can improve complications after amputation, but the mechanism underlying these changes is not yet known (Bragaru et al., 2011, 2015; Wheaton, 2017). Our correlation results may provide a starting point; further research is needed to determine whether active stump activity maintains FC in sensorimotor areas.

The brain as a whole can be viewed as comprising functional networks that interact continuously to maintain complex behavioral routines. Similarly, brain functional changes after amputation are not confined to local circumscribed brain areas that correspond to the amputated limb. Recent amputation studies have shown that sensorimotor areas or networks are coupled to other brain regions or networks. This can explain many of the clinical manifestations after amputation, including pain (Kikkert et al., 2018), emotional impairment (Armstrong et al., 2019), and social impairment (Makin and Flor, 2020). We found a decrease in FC between the dSMN and rFPN, as well as the DAN. The rFPN has been shown to be important in pain processing, somatosensory perception, and activity inhibition, as well as working memory and cognition (Corbetta and Shulman, 2011). The DAN is also called the visuospatial attention network, and underlies hierarchical attention orientation (Vossel et al., 2014). As our knowledge of brain plasticity after amputation deepens, an increasing number of studies have proposed new therapeutic strategies for improving remodeling process to help alleviate postoperative complications, including mirror therapy (Wang et al., 2021), virtual reality (Ambron et al., 2021), and transcranial magnetic stimulation (Pacheco-Barrios et al., 2020).

Plasticity-based therapy has been found to alleviate pain for amputees to some extent; however, the mechanism underlying plasticity-based therapy remains unclear. In the present study, sensorimotor networks were isolated by ICA of fMRI signals. Significant changes in functional connections were found between the vSMN and dSMN, which further demonstrates the diversity of brain remodeling after amputation. This new understanding has potential implications for neurorehabilitation. Clearly, for the rehabilitation of amputees, we not only need to pay attention to the treatment of local cortical areas that have become deafferented by the trauma, but we also need to consider that abnormal changes may occur in brain networks that are distant to the locally affected area. This new understanding of global network changes could inform more comprehensive strategies for amputee rehabilitation. For example, stimulating cortical regions that have become newly connected by plastic afferents invading from the deafferented region could potentially alleviate PLP. Remodeling changes between networks may also play a role in the recovery of amputees.

The present study has some limitations. First, the sample of ULA subjects was small, because it is difficult to recruit these kinds of patients. In future studies, we aim to recruit more ULAs to more reliably control for the time since and level of amputation. Second, the sample size may be affected by bias because the ULAs volunteered for the trial; thus, these amputees might have had more pronounced clinical manifestations and were willing to come to the hospital for treatment solutions. Third, to better understand the pathophysiological processes after amputation, dynamic alterations in multiple networks should have been examined. However, the cross-sectional design of this study means that we were unable to do so. Last, the plasticity process is affected by many factors, including time since amputation and prosthesis use, the effects of which cannot be defined based on the current data. Given these limitations, further studies of upper-limb amputations need to be conducted with larger groups of subjects and over longer periods of time.

Conclusion

Brain plasticity in ULAs is not restricted to local remapping; rather, plasticity occurs at the network level. Inter-network FC alterations are not only observed in the sensorimotor network, but also occur in other neural networks following upper-limb amputation. These findings shed further light on brain plasticity after upper-limb amputation and the mechanisms underlying post-amputation pain.

Author contributions: *XYZ was responsible for study design and manuscript revision. BBB, HFW, and HYZ were responsible for data collection and analysis. BBB, JL, ZBW and YHL were responsible for fMRI data collection. XYH and MXZ supervised fMRI data analysis. BBB was responsible for manuscript writing. All the authors critically reviewed, read and approved the final manuscript.*

Conflicts of interest: *The authors declare that they have no conflicts of interests.*

References

Ambron E, Buxbaum LJ, Miller A, Stoll H, Kuchenbecker KJ, Coslett HB (2021) Virtual reality treatment displaying the missing leg improves phantom limb pain: a small clinical trial. Neurorehabil Neural Repair:15459683211054164.

Armstrong TW, Williamson MLC, Elliott TR, Jackson WT, Kearns NT, Ryan T (2019) Psychological distress among persons with upper extremity limb loss. Br J Health Psychol 24:746-763.

Bao B, Wei H, Luo P, Zhu H, Hu W, Sun Y, Shen J, Zhu T, Lin J, Huang T, Li J, Wang Z, Li Y, Zheng X (2021) Parietal lobe reorganization and widespread functional connectivity integration in upper-limb amputees: A rs-fMRI study. Front Neurosci 15:704079.

Barth AL, Ray A (2019) Progressive circuit changes during learning and disease. Neuron 104:37-46.

Boccia M, Di Vita A, Palermo L, Nemmi F, Traballesi M, Brunelli S, De Giorgi R, Galati G, Guariglia C (2020) Neural modifications in lower limb amputation: an fMRI study on action and non-action oriented body representations. Brain Imaging Behav 14:416-425.

Bragaru M, Dekker R, Geertzen JH, Dijkstra PU (2011) Amputees and sports: a systematic review. Sports Med 41:721-740.

Bragaru M, Dekker R, Dijkstra PU, Geertzen JH, van der Sluis CK (2015) Sports participation of individuals with major upper limb deficiency. Br J Sports Med 49:330-334.

Caspers J, Rubbert C, Eickhoff SB, Hoffstaedter F, Südmeyer M, Hartmann CJ, Sigl B, Teichert N, Aissa J, Turowski B, Schnitzler A, Mathys C (2021) Within- and across-network alterations of the sensorimotor network in Parkinson's disease. Neuroradiology 63:2073-2085.

Chan AW, Bilger E, Griffin S, Elkis V, Weeks S, Hussey-Anderson L, Pasquina PF, Tsao JW, Baker CI (2019) Visual responsiveness in sensorimotor cortex is increased following amputation and reduced after mirror therapy. Neuroimage Clin 23:101882.

Collins KL, Russell HG, Schumacher PJ, Robinson-Freeman KE, O'Conor EC, Gibney KD, Yambem O, Dykes RW, Waters RS, Tsao JW (2018) A review of current theories and treatments for phantom limb pain. J Clin Invest 128:2168-2176.

Corbetta M, Shulman GL (2011) Spatial neglect and attention networks. Annu Rev Neurosci 34:569-599.

Edde M, Leroux G, Altena E, Chanraud S (2021) Functional brain connectivity changes across the human life span: From fetal development to old age. J Neurosci Res 99:236-262.

Flor H, Elbert T, Knecht S, Wienbruch C, Pantev C, Birbaumer N, Larbig W, Taub E (1995) Phantom-limb pain as a perceptual correlate of cortical reorganization following arm amputation. Nature 375:482-484.

Heneka MT, McManus RM, Latz E (2018) Inflammasome signalling in brain function and neurodegenerative disease. Nat Rev Neurosci 19:610-621.

Hortobágyi T, Granacher U, Fernandez-Del-Olmo M, Howatson G, Manca A, Deriu F, Taube W, Gruber M, Márquez G, Lundbye-Jensen J, Colomer-Poveda D (2021) Functional relevance of resistance training-induced neuroplasticity in health and disease. Neurosci Biobehav Rev 122:79-91.

Kikkert S, Johansen-Berg H, Tracey I, Makin TR (2018) Reaffirming the link between chronic phantom limb pain and maintained missing hand representation. Cortex 106:174-184.

Kikkert S, Mezue M, O'Shea J, Henderson Slater D, Johansen-Berg H, Tracey I, Makin TR (2019) Neural basis of induced phantom limb pain relief. Ann Neurol 85:59-73.

Kuffler DP (2018) Origins of Phantom Limb Pain. Mol Neurobiol 55:60-69.

Ledberg A, Akerman S, Roland PE (1998) Estimation of the probabilities of 3D clusters in functional brain images. Neuroimage 8:113-128.

Limakatso K, Bedwell GJ, Madden VJ, Parker R (2020) The prevalence and risk factors for phantom limb pain in people with amputations: A systematic review and meta-analysis. PLoS One 15:e0240431.

Makin TR, Flor H (2020) Brain (re)organisation following amputation: Implications for phantom limb pain. Neuroimage 218:116943.

Makin TR, Scholz J, Filippini N, Henderson Slater D, Tracey I, Johansen-Berg H (2013) Phantom pain is associated with preserved structure and function in the former hand area. Nat Commun 4:1570.

Makin TR, Filippini N, Duff EP, Henderson Slater D, Tracey I, Johansen-Berg H (2015) Network-level reorganisation of functional connectivity following arm amputation. Neuroimage 114:217-225.

McKechnie PS, John A (2014) Anxiety and depression following traumatic limb amputation: a systematic review. Injury 45:1859-1866.

McKeown MJ, Sejnowski TJ (1998) Independent component analysis of fMRI data: examining the assumptions. Hum Brain Mapp 6:368-372.

Melzack R (2001) Pain and the neuromatrix in the brain. J Dent Educ 65:1378-1382.

Nardone R, Versace V, Sebastianelli L, Brigo F, Christova M, Scarano GI, Saltuari L, Trinka E, Hauer L, Sellner J (2019) Transcranial magnetic stimulation in subjects with phantom pain and non-painful phantom sensations: A systematic review. Brain Res Bull 148:1-9.

Pacheco-Barrios K, Pinto CB, Saleh Velez FG, Duarte D, Gunduz ME, Simis M, Lepesteur Gianlorenco AC, Barouh JL, Crandell D, Guidetti M, Battistella L, Fregni F (2020) Structural and functional motor cortex asymmetry in unilateral lower limb amputation with phantom limb pain. Clin Neurophysiol 131:2375-2382.

Peraza LR, Nesbitt D, Lawson RA, Duncan GW, Yarnall AJ, Khoo TK, Kaiser M, Firbank MJ, O'Brien JT, Barker RA, Brooks DJ, Burn DJ, Taylor JP (2017) Intra- and inter-network functional alterations in Parkinson's disease with mild cognitive impairment. Hum Brain Mapp 38:1702-1715.

Power JD, Mitra A, Laumann TO, Snyder AZ, Schlaggar BL, Petersen SE (2014) Methods to detect, characterize, and remove motion artifact in resting state fMRI. Neuroimage 84:320-341.

Qureshi MK, Ghaffar A, Tak S, Khaled A (2020) Limb salvage versus amputation: a review of the current evidence. Cureus 12:e10092.

Sherman RA, Sherman CJ, Parker L (1984) Chronic phantom and stump pain among American veterans: results of a survey. Pain 18:83-95.

Smith SM, Fox PT, Miller KL, Glahn DC, Fox PM, Mackay CE, Filippini N, Watkins KE, Toro R, Laird AR, Beckmann CF (2009) Correspondence of the brain's functional architecture during activation and rest. Proc Natl Acad Sci U S A 106:13040-13045.

Smitha KA, Akhil Raja K, Arun KM, Rajesh PG, Thomas B, Kapilamoorthy TR, Kesavadas C (2017) Resting state fMRI: A review on methods in resting state connectivity analysis and resting state networks. Neuroradiol J 30:305-317.

Stankevicius A, Wallwork SB, Summers SJ, Hordacre B, Stanton TR (2021) Prevalence and incidence of phantom limb pain, phantom limb sensations and telescoping in amputees: A systematic rapid review. Eur J Pain 25:23-38.

Vossel S, Geng JJ, Fink GR (2014) Dorsal and ventral attention systems: distinct neural circuits but collaborative roles. Neuroscientist 20:150-159.

Wall JT, Xu J, Wang X (2002) Human brain plasticity: an emerging view of the multiple substrates and mechanisms that cause cortical changes and related sensory dysfunctions after injuries of sensory inputs from the body. Brain Res Brain Res Rev 39:181-215.

Wang D, Qin W, Liu Y, Zhang Y, Jiang T, Yu C (2014) Altered resting-state network connectivity in congenital blind. Hum Brain Mapp 35:2573-2581.

Wang F, Zhang R, Zhang J, Li D, Wang Y, Yang YH, Wei Q (2021) Effects of mirror therapy on phantom limb sensation and phantom limb pain in amputees: A systematic review and meta-analysis of randomized controlled trials. Clin Rehabil 35:1710-1721.

Wheaton LA (2017) Neurorehabilitation in upper limb amputation: understanding how neurophysiological changes can affect functional rehabilitation. J Neuroeng Rehabil 14:41.

Yang J, Gohel S, Vachha B (2020) Current methods and new directions in resting state fMRI. Clin Imaging 65:47-53.

Yang N, Waddington G, Adams R, Han J (2018) Translation, cultural adaption, and test-retest reliability of Chinese versions of the Edinburgh Handedness Inventory and Waterloo Footedness Questionnaire. Laterality 23:255-273.

Zhan Y, Ma J, Alexander-Bloch AF, Xu K, Cui Y, Feng Q, Jiang T, Liu Y (2016) Longitudinal study of impaired intra- and inter-network brain connectivity in subjects at high risk for Alzheimer's disease. J Alzheimers Dis 52:913-927.

Zhao Z, Wu J, Fan M, Yin D, Tang C, Gong J, Xu G, Gao X, Yu Q, Yang H, Sun L, Jia J (2018) Altered intra- and inter-network functional coupling of resting-state networks associated with motor dysfunction in stroke. Hum Brain Mapp 39:3388-3397.

C-Editor: Zhao M; S-Editor: Li CH; L-Editors: Li CH, Song LP; T-Editor: Jia Y